Asociación Argentina de Mecánica Computacional

Mecánica Computacional Vol XXIX, págs. 673-682 (artículo completo)
Eduardo Dvorkin, Marcela Goldschmit, Mario Storti (Eds.)
Buenos Aires, Argentina, 15-18 Noviembre 2010

NUMERICAL ASPECTS ON THE COMPUTATION OF ORTHOTROPIC THICK PLATE

Adriana dos Reis and Éder L. de Albuquerque

Faculty of Technology, Department of Mechanical Engineering, University of Brasília - UnB, Campus Universitário Darcy Ribeiro, Asa Norte Brasília, Brasil, adriana@fem.unicamp.br, eder@unb.br, http://www.unb.br

Keywords: Orthotropic fundamental solutions, Thick plates, Boundary element method, Telles transformation.

Abstract. Fundamental solutions for bending of orthotropic thick plates are obtained using Hörmander operator and Radon transform. So, they do not have a closed form and numerical integration is necessary to compute fundamental solutions in each field point. In this paper an analysis of the fundamental solution for orthotropic thick plate is presented. Integration aspects are taking into account. It is discussed different approaches in order to carry out the numerical integration in a fast and accurate way. An analysis of computer cost is presented and some results are compared with literature.

1 INTRODUCTION

In the case of laminates composite, the difference between the properties elastic fiber and matrix, results in most applications, in a high ratio between the modulus of elasticity in the direction of the fibers and the modulus of shear in the transverse direction. Therefore, the deformation due to shear can be significant even in thin plates. Thus, theories that take into account the transverse shear deformation are more suitable for modeling. The first paper on the boundary element analysis of thick Reissner plates was introduced by Weeën (1982), who employed the Hörmander method for the derivation of the fundamental solution. Barcellos and Silva (1989) used similar formulations to treat Mindlin's model. After the original works of Weeën (1982), many references have reported the application of boundary elements to bending analysis of thick plates, most of them using the Reissner model as, for example, Karam and Telles (1988), Long et al. (1988), Katsikadelis and Yotis (1993), Yan (1995), and Rashed et al. (1997). A field decomposition was presented by Palermo Jr. (2003) to obtain a boundary element formulation for the classical model (Kirchhoff plates) from that used for the Reissner-Mindlin one. As we can see, a large number of articles with the analysis of isotropic plates can be found in literature. However, only few works can be found with the analysis of orthotropic plates. Wang and Huang (1991) presented a boundary element method of moderately thick orthotropic plates. In Wang and Schweizerhof (1996) the previous formulation was extended to laminated composites. This work presents a boundary element formulation for orthotropic thick plates. It uses the fundamental solution proposed by Wang and Huang (1991) that takes into account the effects of shear deformation and was derived by means of Hörmander operator and the Radom transform. Domain integrals which come from transversal applied loads are exactly transformed into boundary integrals by a radial integration technique and is used the Telles transformation (Telles, 1987) for treat singular or nearly singular integrals. Some numerical examples concerning orthotropic plate bending problems are analyzed with the BEM.

2 DIFFERENTIAL EQUATIONS OF EQUILIBRIUM

Equations of equilibrium for the plate are given by:

$$\begin{aligned} M_{\alpha\beta,\beta} - Q_\alpha &= 0, \\ Q_{\alpha,\alpha} + q &= 0, \end{aligned} \tag{1}$$

where q is the distributed transverse load per unit area in the x_3 direction. $M_{\alpha\beta}$ are the moments and, Q_α are the shear forces that relate displacements and slopes by:

$$\begin{aligned} M_{\alpha\beta} &= D_{\alpha\beta}(U_{\alpha,\beta} + U_{\beta,\alpha}) + C_{\alpha\beta}U_{\gamma,\gamma}, \\ Q_\alpha &= C_\alpha(U_{3,\alpha} + U_\alpha), \end{aligned} \tag{2}$$

where U_α are the rotations and U_3 is the deflection in the thickness direction. Throughout the formulations Greek indices take values of 1 and 2, and Latin indices 1, 2 and 3.

The generalized Navier equations can be formed by substituting the values of the constants into the equilibrium equations (1) and (1) to give:

$$L_{ij}U_j + b_i = 0, \tag{3}$$

in which

$$L_{11}=D_{11}\frac{\partial^2}{\partial x_1^2}+D_{66}\frac{\partial^2}{\partial x_2^2}-C_1,\qquad L_{22}=D_{66}\frac{\partial^2}{\partial x_1^2}+D_{22}\frac{\partial^2}{\partial x_2^2}-C_2,$$
$$L_{12}=L_{21}=(D_{11}\nu_{yx}+D_{66})\frac{\partial^2}{\partial x_1\partial x_2},\qquad L_{13}=-L_{31}=-C_1\frac{\partial}{\partial x_1},\tag{4}$$
$$L_{23}=-L_{32}=-C_2\frac{\partial}{\partial x_2},\qquad L_{33}=C_1\frac{\partial^2}{\partial x_1^2}+C_2\frac{\partial^2}{\partial x_2^2},$$

where b_i represents 0, 0, q, respectively, L_{ij} is the generalized Navier differential operator. The values of the constants are found to be:

$$C_{12}=C_{21}=0,\qquad C_{11}=D_{11}\nu_{yx},\qquad C_{22}=D_{22}\nu_{xy},$$
$$D_{11}=\frac{E_xh^3}{12(1-\nu_{xy}\nu_{yx})},\quad D_{22}=\frac{E_yh^3}{12(1-\nu_{xy}\nu_{yx})},\quad D_{66}=\frac{G_{xy}h^3}{12},\tag{5}$$
$$D_{11}\nu_{yx}=D_{22}\nu_{xy},\qquad C_1=G_{zx}kh,\qquad C_2=G_{zy}kh,$$

where E_x and E_y are elastic moduli; ν_{xy} and ν_{yx} are Poisson ratios; G_{xy}, G_{zx}, and G_{zy} are shear moduli; h is the thickness of the plate, and $k=5/6$.

3 FUNDAMENTAL SOLUTIONS

The fundamental solutions of the orthotropic thick plate taking into account the transverse shear deformation are a set of particular solutions of the differential Eq. (3) under a unit concentrated load, i.e., the solutions satisfy the following inhomogeneous differential equations:

$$L_{ij}^{adj}U_{kj}^*(\zeta,x)=-\delta(\zeta,x)\delta_{ki},\tag{6}$$

in which $\delta(\zeta,x)$ denotes the Dirac delta function, ζ represents the source point, x is a field point, and L_{ij}^{adj} is the adjoint operator (see Wang and Huang (1991)). Following Hörmander's operator method, the solutions of Eq. (3) can be written as:

$$U_{ij}^*(\zeta,x)={}^{co}L_{ji}^{adj}\phi(\zeta,x),\tag{7}$$

where $\phi(\zeta,x)$ is a unknown scalar function and ${}^{co}L_{ji}^{adj}$ is the cofactor matrix of the operator L_{ji}^{adj} that is given by:

$$\begin{aligned}{}^{co}L_{\alpha\beta}^{adj}&=E_{\alpha\beta}\nabla^2\nabla_k^2-B_{\alpha\beta}\frac{\partial^2}{\partial x_\alpha\partial x_\beta}-C_1C_2\frac{\partial^2}{\partial x_\alpha\partial x_\beta},\\ {}^{co}L_{3\alpha}^{adj}&=-{}^{co}L_{\alpha3}^{adj}=\frac{\partial}{\partial x_\alpha}(E_{\alpha3}\frac{\partial^2}{\partial x_2^2}+B_{\alpha3}\frac{\partial^2}{\partial x_1^2}-C_1C_2),\\ {}^{co}L_{33}^{adj}&=D_{11}D_{66}\frac{\partial^4}{\partial x_1^4}+(D_{11}D_{22}-D_{11}^2\nu_{yx}^2-2D_{11}D_{66}\nu_{yx})\frac{\partial^4}{\partial x_1^2\partial x_2^2}+\\ &\quad+D_{22}D_{66}\frac{\partial^4}{\partial x_2^4}-(D_{11}C_2+C_1D_{66})\frac{\partial^2}{\partial x_1^2}-(C_1D_{22}+C_2D_{66})\frac{\partial^2}{\partial x_2^2}+C_1C_2.\end{aligned}\tag{8}$$

The following symbols have been introduced:

$$\begin{aligned}
&B_{11} = D_{21} - D_{66}, && B_{22} = D_{11} - D_{66}, && E_{11} = D_{22},\\
&B_{12} = B_{21} = (D_{11}\nu_{yx} + D_{66}), && E_{22} = D_{11}, && E_{12} = E_{21} = 0,\\
&E_{13} = C_1 D_{22} - C_2(D_{11}\nu_{yx} + D_k), && B_{13} = C_1 D_{66}, && E_{23} = C_2 D_{66},\\
&B_{23} = C_2 D_{11} - C_1(D_{11}\nu_{yx} + D_{66}), && \nabla_k^2 = C_1 \tfrac{\partial^2}{\partial x_1^2} + C_2 \tfrac{\partial^2}{\partial x_2^2}, && \nabla^2 = \tfrac{\partial^2}{\partial x_1^2} + \tfrac{\partial^2}{\partial x_2^2}.
\end{aligned} \tag{9}$$

Now, the potential $\phi(\zeta, x)$ can be evaluated as follows:

$$det[^{co}L_{\alpha\beta}^{adj}]\phi(\zeta, x) = -\delta(\zeta, x). \tag{10}$$

By the above procedure, the derivation of the fundamental solution of Eq. (6) is reduced to that of Eq. (10). As soon as the solution of Eq. (10) is obtained, substituting it into Eq. (7) and by differentiation we can get the solutions of Eq. (6). Eq. (10) is a sixth order partial differential equation. Using the plane wave decomposition method, the partial differential Eq. (10) can be reduced to an ordinary differential equation, which simplifies the treatment of the problem. We first expand $\delta(\zeta, x)$ into a plane wave (see, for example, Wang and Huang (1991)):

$$\delta(\zeta, x) = -\frac{1}{4\pi^2} \int_0^{2\pi} \mid \omega_1(x - \zeta) + \omega_2(y - \eta) \mid^{-2} d\theta, \tag{11}$$

in which (ω_1, ω_2) are the coordinates of a point on the unit circle, i.e., $\omega_1 = \cos(\theta)$, $\omega_2 = \sin(\theta)$, (x, y) and (ζ, η) are the coordinates of a field point and a source point, respectively. Similarly, $\phi(\zeta, x)$ can be written as:

$$\phi(\zeta, x) = \int_0^{2\pi} \varphi(\rho) d\theta, \tag{12}$$

where $\rho = \omega_1(x - \zeta) + \omega_2(y - \eta)$, $\varphi(\rho)$ is a function depending only on ρ.

By substituting Eq. (11) and Eq. (12) into Eq. (10), and considering differential relationship $\frac{\partial}{\partial x_\alpha} = \omega_\alpha \frac{d}{d\rho}$, we obtain the following equation:

$$\frac{d^4}{d\rho^4}\left(\frac{d^2}{d\rho^2} - p^2\right)\varphi(\rho) = \frac{1}{4\pi^2 a^2} \mid \rho \mid^{-2}, \tag{13}$$

in which
$a^2 = C_1 D_{11} D_{66} \omega_1^6 + C_1(D_{11}D_{22} - D_{11}^2\nu_{yx}^2 - 2D_{11}D_{66}\nu_{yx})\omega_1^4\omega_2^2 + C_1 D_{22} D_{66}\omega_1^2\omega_2^4 +$
$+ C_2 D_{11} D_{66}\omega_1^4\omega_2^2 + C_2 D_{22} D_{66}\omega_2^6 + C_2(D_{11}D_{22} - D_{11}^2\nu_{yx}^2 - 2D_{11}D_{66}\nu_{yx})\omega_1^2\omega_2^4$,
$b^2 = C_1 C_2[D_{11}\omega_1^4 + 2(2D_{66} + D_{11}\nu_{yx})\omega_1^2\omega_2^2 + D_{22}\omega_2^4]$,
$p^2 = b^2/a^2$.

The solution of Eq. (10) is now reduced to solve the ordinary differential Eq. (13). After four times integration of Eq. (13) and leaving out the constants of integration, we obtain:

$$\frac{d^2\varphi(\rho)}{d\rho^2} - p^2\varphi(\rho) = -\frac{1}{8\pi^2 a^2} p^2 \log \mid \rho \mid . \tag{14}$$

The solution of Eq. (14) can be written as follows:

$$\varphi(\rho) = f_1(\rho)\exp(p\rho) + f_2(\rho)\exp(-p\rho). \tag{15}$$

By the method of variation of parameters, the coefficients $f_1(\rho)$ and $f_2(\rho)$ can be obtained. By substituting $f_1(\rho)$ and $f_2(\rho)$ into Eq. (15), we obtain:

$$\begin{aligned}\varphi(\rho) &= \frac{1}{8\pi^2 p^4 a^2}\Bigg[p^2\rho^2 \log\mid\rho\mid + 2\log\mid\rho\mid + 3 + \exp(p\rho)\int_\rho^\infty \frac{\exp(-p\sigma)}{\sigma}d\sigma + \\ &\quad - \exp(-p\rho)\int_{-\infty}^{\rho}\frac{\exp(p\sigma)}{\sigma}d\sigma\Bigg]. \end{aligned} \tag{16}$$

Substituting Eq. (16) into Eq. (12) and integrating, we can obtain the function $\Phi(\zeta, x)$. The generalized displacement and boundary tractions can be expressed in the following forms:

$$\begin{aligned} U^*_{ij}(\zeta, x) &= \int_0^{2\pi} \tilde{U}_{ij}(\rho)d\theta, \\ P^*_{ij}(\zeta, x) &= \int_0^{2\pi} \tilde{P}_{ij}(\rho)d\theta. \end{aligned} \tag{17}$$

Details of the implementation of equations (17) can be found in Wang and Huang (1991).

3.1 Integration of fundamental solutions

It can be seen in equations (17) that, in order to obtain fundamental solutions U^*_{ij} and P^*_{ij}, it is necessary to integrate $\tilde{U}_{ij}$ and $\tilde{P}_{ij}$. As its is carried out numerically, the way in which this integrals are computed is a key point in the performance of the boundary element code. Figures 1 to 6 show the behaviour of kernels $\tilde{U}_{ij}$ and $\tilde{P}_{ij}$, considering as source point $\zeta = 0.5$, $\eta = 0$, and as field point $x = 0$ and $y = 0.0094$. The material properties are $E_L = 20.0485$ GPa; $E_T = 6.0039$ GPa; $G_{LT} = 0.5$ GPa; $G_{TT} = 0.2$ GPa; $\nu_{LT} = 0.0417$; $h = 0.25$ m, and componentes of normal vector are $n_1 = -1$ and $n_2 = 0$.

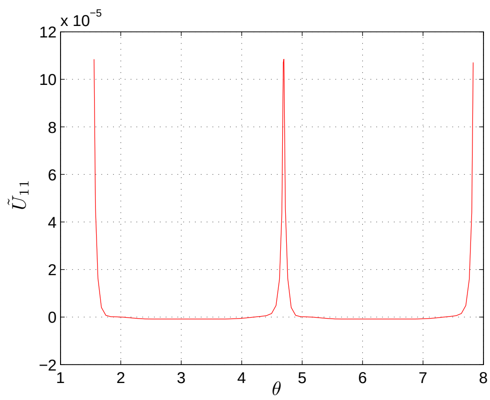

Figure 1: $\tilde{U}_{11}$

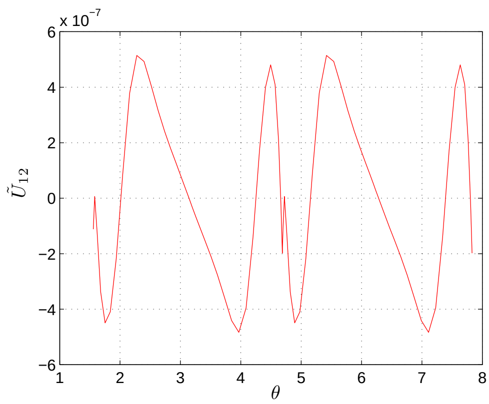

Figure 2: $\tilde{U}_{12}$

Figures 1 to 6 show that all kernels are symmetric in relation to $\theta_0 = \arctan\left(-\frac{x-\zeta}{y-\eta}\right)$. So, it is necessary to carried out integration just in half of the interval $[0, 2\pi]$. On the other hand, it can be seen that all kernels are functions that are very difficult to integrate because some of them present singular behaviour near θ_0 and oscillaions in the integration interval. Although these graphics are for a specific problem, similar behaviour is found in other problems.

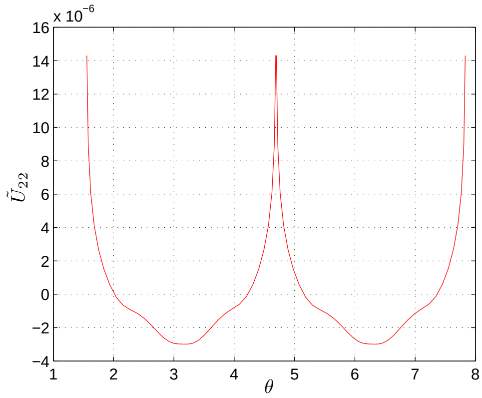

Figure 3: $\tilde{U}_{22}$

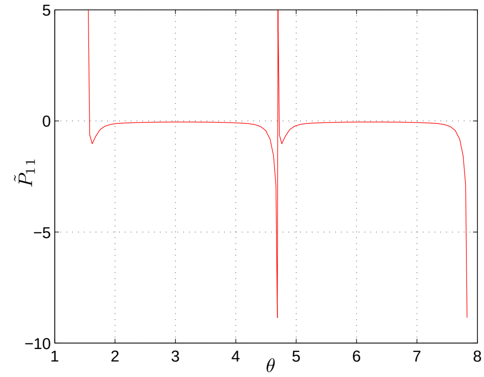

Figure 4: $\tilde{P}_{11}$

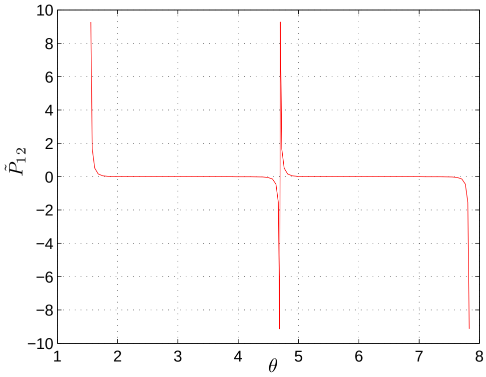

Figure 5: $\tilde{P}_{12}$

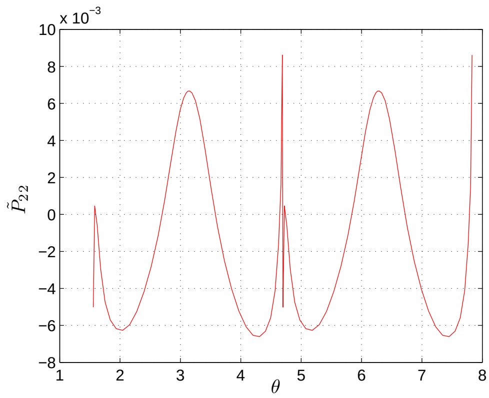

Figure 6: $\tilde{P}_{22}$

In this work, two approaches are used to compute integrals of equation (17). In the first one, standard Gauss point quadrature is used. In second, Telles transformation is used in order to concentrate integration points near singularity. A brief description of Telles transformation is given in the next section.

4 TELLES TRANSFORMATION

Telles (1987) introduce an efficient mean of computing singular or nearly singular integrals found in two-dimensional, axisymmetric and three-dimensional boundary element applications. Emphasis is given to a new third degree polynomial transformation which was found greatly to improve the accuracy of Gaussian quadrature schemes within the near-singularity range. The procedure can easily be implemented into boundary element codes and presents the important feature of being self-adaptive, i.e., it produces a variable that depends on the minimum distance from the source point to the element. The self-adaptiveness of the scheme also makes it inactive when not useful (large source distances) which makes it very safe for general usage.

Consider the integral:

$$I = \int_{-1}^{1} f(\eta) d\eta, \tag{18}$$

in which $f(\eta)$ is singular at a point $\bar{\eta}$.

The idea is to transform the coordinates η to γ where the jacobian $\frac{d\eta}{d\gamma}$ vanishes at the point $\bar{\eta}$ where $f(\eta)$ is singular.

In this article, it is choosen a third-degree relation:

$$\eta(\gamma) = a\gamma^3 + b\gamma^2 + c\gamma + d, \tag{19}$$

such that the following requirements are met:

$$\begin{aligned} \frac{d^2\eta}{d\gamma^2}|_{\bar{\eta}} &= 0, \\ \frac{d\eta}{d\gamma}|_{\bar{\eta}} &= 0, \\ \eta(1) &= 1, \\ \eta(-1) &= -1. \end{aligned} \tag{20}$$

Thus, expression becomes (18)

$$I = \int_{-1}^{1} f\{[(\gamma-\bar{\gamma})^3 + \bar{\gamma}(\bar{\gamma}^2+3)]/(1+3\bar{\gamma}^2)\}3(\gamma-\bar{\gamma}^2)/(1+3\bar{\gamma}^2)d\gamma, \tag{21}$$

where $\bar{\gamma}$ is simply the value of γ which satisfies $\eta(\bar{\gamma}) = \bar{\eta}$; this parameter can be calculated by:

$$\bar{\gamma} = \sqrt[3]{(\bar{\eta}\eta^* + |\eta^*|)} + \sqrt[3]{(\bar{\eta}\eta^* - |\eta^*|)} + \eta, \tag{22}$$

and $\eta^* = \bar{\eta}^2 - 1$.

5 BOUNDARY INTEGRAL EQUATIONS

The integral equation can be derived by considering the integral representation of the governing Eq.(1) via the following integral identity:

$$\int_{\Omega} [(M_{\alpha\beta,\beta} - Q_\alpha)U^*_\alpha + (Q_{\alpha,\alpha} + q)U^*_3]d\Omega = 0, \tag{23}$$

where $U^*_i (i = \alpha, 3)$ are the weighting functions. Integrating by parts (applying Green's second identity) and making use of the algebraic relationships, it gives:

$$U_j(\zeta) + \int_\Gamma P^*_{ij}(\zeta,x)U_j(x)d\Gamma = \int_\Gamma U^*_{ij}(\zeta,x)P_j(x)d\Gamma + \int_\Omega q(x)U^*_{i3}(\zeta,x)d\Omega. \tag{24}$$

By taking the point ζ to the boundary at the position $\zeta \in \Gamma$, Eq. (24) can be written as:

$$c_{ij}(\zeta)U_j(\zeta) + \fint_\Gamma P^*_{ij}(\zeta,x)U_j(x)d\Gamma = \int_\Gamma U^*_{ij}(\zeta,x)P_j(x)d\Gamma + \int_\Omega q(x)U^*_{i3}(\zeta,x)d\Omega, \tag{25}$$

where $\fint$ denotes a Cauchy Principal Value integral, $\zeta, x \in \Gamma$ are source point and field point, respectively. The value of $c_{ij}(x)$ is equal to $\delta_{ij}/2$ when x is located on a smooth boundary. Equation (25) represents three integral equations, two ($i = \alpha = 1, 2$) for rotations and one ($i = 3$) for deflection. The last integral on the right hand side of equation (25), that is a domain integral, is transformed into a boundary integral using the procedures presented by Albuquerque et al. (2006).

6 MODELING SYMMETRIC CROSS-PLY LAMINATES

Although the formulation presented in this paper is for single layer orthotropic material, symmetric crossply laminates can be also modeled using equivalent global stiffness constants. The bending stiffiness matrix of a laminate composite is given by:

$$\mathbf{D} = \sum \overline{\mathbf{Q_k}}(t_k^3 - t_{k-1}^3), \tag{26}$$

where

$$\overline{\mathbf{Q_k}} = \mathbf{T^{-1}}\mathbf{Q}(\mathbf{T^{-1}})^{-1}, \tag{27}$$

$$\mathbf{Q} = \begin{bmatrix} Q_{11} & Q_{12} & 0 \\ Q_{12} & Q_{22} & 0 \\ 0 & 0 & Q_{66} \end{bmatrix}, \tag{28}$$

and

$$\begin{array}{ll} Q_{11} = E_L/(1-\nu_{LT}\nu_{TL}), & Q_{22} = E_T/(1-\nu_{LT}\nu_{TL}), \\ Q_{66} = G_{LT}, & Q_{16} = Q_{26} = 0, \\ Q_{12} = \nu_{TL}E_L/(1-\nu_{LT}\nu_{TL}) = \nu_{LT}E_2/(1-\nu_{LT}\nu_{TL}). & \end{array} \tag{29}$$

The inverse of $\mathbf{D}$ is the $\mathbf{S}$ matrix given by:

$$\mathbf{S} = \mathbf{D^{-1}} = \frac{12}{h^3}\begin{bmatrix} 1/E_L^* & -\nu_{21}/E_T^* & 0 \\ -\nu_{12}/E_L^* & 1/E_T^* & 0 \\ 0 & 0 & 1/G_{LT}^* \end{bmatrix}, \tag{30}$$

where E_L^*, E_T^*, ν_{LT}, ν_{TL} and G_{LT}^* are the equivalent material properties of the symmetric cross ply laminates, t is total thickeness of the laminate.

From equation (30) we can obtain:

$$\begin{aligned} E_L^* &= 1/S_{11}, \\ E_T^* &= 1/S_{22}, \\ G_{LT}^* &= 1/S_{33}, \\ \nu_{LT}^* &= -S_{12}E_L^*. \end{aligned} \tag{31}$$

7 NUMERICAL RESULTS

To validate the procedures implemented and to assess the accuracy of solutions, consider a square plate of simply supported boundary with five layers $[0^o/90^o/0^0/90^o/0^0]$ subjected to a sinusoidally distributed load $g = g_o\sin(\frac{\pi x}{a})\sin(\frac{\pi y}{b})$ and, $a/t = 10$, $a/t = 20$ and $a/t = 100$. The material constants are $E_L = 25$ GPa, $E_T = 1$ GPa, $G_{LT} = 0.5$ GPa, $G_{TT} = 0.2$ GPa, $\nu_{LT} = 0.25$. Results are compared with Ghosh and Dey (1992) e Pagano and Hatfield (1972), as shown in Table (1). The laminate is discretized into two discontinuous quadratic elements per side. Where $\hat{w} = w\pi^4 Q/(12g_o tS^4)$ and $Q = 4G_{LT} + \{E_L + E_T(1+2\nu_{LT})\}/(1-\nu_{LT}\nu_{TL})$.

The displacement at the central point of the plate is shown in Table 1. In this table, $\hat{w_T}$ is the solution obtained by Telles Transformation with 20 integration points; ref1. is the result of Pagano and Hatfield (1972); ref2. is the result of Ghosh and Dey (1992); $\hat{w_{g1}}$ is the solution computed by standard Gauss Quadrature with 20 integration points and $\hat{w_{g2}}$ is the solution computed by standard Gauss Quadrature with 80 integration points.

We can see that there is a good agreement among results from literature, displacements computed using standard Gauss quadrature with 80 integration points, and Telles transformation with 20 integration points. On the other hand, the agreement of the displacement obtained by standard Gauss quadrature using 20 integration points is very poor.

We can conclude that the use of Telles transformation strongly reduces the amount of integration points necessary to obtain accurate results.

$S = a/t$	$\hat{w_T}$	$\hat{w}$(ref1.)	$\hat{w}$(ref2.)	$\hat{w_{g1}}$	$\hat{w_{g2}}$
10	1.42	1.57	1.42	1.49	1.43
20	1.11	1.15	1.10	3.35	1.14
100	1.01	1.01	1.01	0.59	-0.11

Table 1: Center deflection of the orthotropic thick square plate of simply supported boundary with five layers.

8 CONCLUSIONS

This paper presented a boundary element formulation for orthotropic thick plates. The fundamental solution was derived by means of Hörmander operator and the Radom transform. Kernels of fundamental solutions were integrated by standard Gauss quadrature and Telles transformation. It has been shown that the use of Telles tranformation strongly reduces the amount of integration points necessary to obtain accurate results.

9 ACKNOWLEDGEMENTS

The authors would like to thank the National Council for Scientific and Technological Development (CNPq) for financial support of this work .

REFERENCES

Albuquerque E., Sollero P., Venturini W., and Aliabadi M. Boundary element analysis of anisotropic Kirchhoff plates. *International Journal of Solids and Structures*, 43:4029–4046, 2006.

Barcellos C. and Silva L. A boundary element formulation for the Mindlin's plate model. *Boundary element techniques: applications in stress analysis and heat transfer*, pages 122–130, 1989.

Ghosh A. and Dey S. A simple fiite elemet for the analysis of laminated plates. *Computers and Structures*, 44:585–596, 1992.

Karam V. and Telles J. On boundary elements for Reissner's plate theory. *Engineering Analysis with Boundary Elements*, 5:21–27, 1988.

Katsikadelis J. and Yotis A. A new boundary element solution of thick plates modeled by Reissner's theory. *Engineering Analysis with Boundary Elements*, 12:65–74, 1993.

Long S., Brebbia C., and Telles J. Boundary element bending analysis of moderately thick plates. *Engineering Analysis with Boundary Elements*, 5:64–74, 1988.

Pagano N. and Hatfield S. Elastic behaviour of multilayered bidirectional composites. *AIAA Joural*, 10:931–933, 1972.

Palermo Jr. L. Plate bending analysis using the classical or the Reissner-Mindlin models. *Engineering Analysis with Boundary Elements*, 27:603–609, 2003.

Rashed Y., Aliabadi M., and Brebbia C. On the evaluation of the stresses in the bem for reissner plate-bending problems. *Applied Mathematical Modelling*, 21:155–163, 1997.

Telles J. A self-adaptive co-ordinate transformation for efficient numerical evaluation of general boundary element integrals. *International Journal for Numerical Methods in Engineering*, 24:959–973, 1987.

Wang J. and Huang M. Boundary element method for orthotropic thick plates. *Acta Mechanica Sinica*, 7:258–266, 1991.

Wang J. and Schweizerhof K. Fundamental solutions and boundary integral equations of moderately thick symmetrically laminated anisotropic plates. *Communications in Numerical Methods in Engineering*, 12:383–394, 1996.

Weeën V.F. Application of the boundary integral equation method to Reissner's plate model. *International Journal for Numerical Methods in Engineering*, 18:1–10, 1982.

Yan X. A new bem approach for Reissner's plate bending. *Computers and Structures*, 54:1085–1090, 1995.